

10.24425/acs.2019.129387

Archives of Control Sciences
Volume 29(LXV), 2019
No. 2, pages 387–408

Tracking control for a cascade perturbed control system using the active disturbance rejection paradigm

RADOSŁAW PATELSKI and DARIUSZ PAZDERSKI

In this paper the stability of a closed-loop cascade control system in the trajectory tracking task is addressed. The considered plant consists of underlying second-order fully actuated perturbed dynamics and the first order system which describes dynamics of the input. The main theoretical result establishes the conditions for Lyapunov stability formulated for the perturbed cascade control structure taking advantage of the active rejection disturbance approach. In particular, limitations imposed on a feasible set of an observer bandwidth are discussed. In order to illustrate characteristics of the closed-loop control system simulation results are presented. Furthermore, the particular implementation of the cascade control algorithm is verified experimentally using a two-axis telescope mount. The obtained results confirm that the considered control strategy can be efficiently applied for a class of mechanical systems when a high position tracking precision is required.

Key words: active disturbance rejection, cascade control systems, stability of perturbed systems, high-precision tracking control, control of astronomical mounts

1. Introduction

Set-point regulation and trajectory tracking constitute elementary tasks in control theory. It is well known that a fundamental method of stabilisation by means of a smooth static state feedback has significant limitations which come, among others, from the inability to measure the state as well as the occurrence of parametric and structural model uncertainties. Thus, for these reasons, various adaptive and robust control techniques are required to improve the performance of the closed-loop system. In particular, algorithms used for the state and disturbance estimation are of great importance here.

The use of high gain observers (HGOs) is well motivated in the theory of linear dynamic systems, where it is commonly assumed that state estimation

Authors are with the Poznań University of Technology, Institute of Automation and Robotics, ul. Piotrowo 3a, 60-965 Poznań, Poland.

This work was supported by the National Science Centre (NCN) under the grant No. 2014/15/B/ST7/00429, contract No. UMO-2014/15/B/ST7/00429.

Received 18.01.2019. Revised 15.05.2019.

dynamics are negligible with respect to the dominant dynamics of the closed-loop system. A similar approach can be employed successfully for a certain class of nonlinear systems where establishing a fast convergence of estimation errors may be sufficient to ensure the stability, [15]. In a natural way, the HGO observer is a basic tool to support a control feedback when a plant model is roughly known. Here one can mention the free-model control paradigm introduced by Fliess and others, [7, 8] as well as the active disturbance rejection control (ADRC) proposed by Han and Gao, [11–14].

It turns out that the above-mentioned control methodology can be highly competitive with respect to the classic PID technique in many industrial applications, [6, 19, 20, 22, 24, 26]. Furthermore, it can be regarded as an alternative control approach in comparison to the sliding control technique proposed by Utkin and others, [3, 25], where bounded matched disturbances are rejected due to fast switching discontinuous controls. Thus, it is possible to stabilise the closed-loop control system, in the sense of Filippov, on a prescribed, possibly time-varying, sliding surface, [4, 21]. Currently, also second and higher-order sliding techniques for control and state estimations are being explored, [2, 5, 17, 18]. It is noteworthy to recall a recent control algorithm based on higher-order sliding modes to solve the tracking problem in a finite time for a class of uncertain mechanical systems in robotics, [9, 10].

From a theoretical point of view, some questions arise regarding conditions of application of control techniques based on a disturbance observer, with particular emphasis on maintaining the stability of the closed-loop system. Recently, new results concerning this issue have been reported for ADRC controllers, [1, 23]. In this paper we further study the ADRC methodology taking into account a particular structure of perturbed plant. Basically, we deal with a cascade control system which is composed of two parts. The first component is represented by second-order dynamics which constitute an essential part of the plant. It is assumed that the system is fully actuated and subject to matched-type disturbances with bounded partial derivatives. The second component is defined by an elementary first-order linear system which describes input dynamics of the entire plant. Simultaneously, it is supposed that the state and control input of the second order dynamics are not fully available.

It can be seen that the considered plant well corresponds to a class of mechanical systems equipped with a local feedback applied at the level of actuators. As a result of additional dynamics, real control forces are not accessible directly which may deteriorate the stability of the closed-loop system.

In order to analyse the closed-loop system we take advantage of Lyapunov tools. Basically, we investigate how an extended state observer (ESO) affects the stability when additional input dynamics are considered. Further we formulate stability conditions and estimate bounds of errors. In particular, we show that the observer gains cannot be made arbitrarily large as it is commonly recommended

in the ADRC paradigm. Such an obstruction is a result of the occurrence of input dynamics which is not explicitly taken into account in the feedback design procedure.

According to the best authors' knowledge, the Lyapunov stability analysis for the considered control structure taking advantage of the ADRC approach has not been addressed in the literature so far.

Theoretical results are: active disturbance rejection, cascade control systems, stability of perturbed systems, high-precision tracking control, control of astronomical mounts – illustrated by numerical simulations and experiments. The experimental validation are conducted on a real two-axis telescope mount driven by synchronous gearless motors, [16]. Here we show that the considered methods provide high tracking accuracy which is required in such an application. Additionally, we compare the efficiency of compensation terms, computed based on the reference trajectory and on-line estimates in order to improve the tracking performance.

The paper is organised as follows. In Section 2 the model of a cascade control process is introduced. Then a preliminary feedback is designed and a corresponding extended state observer is proposed. The stability of the closed-loop system is studied using Lyapunov tools and stability conditions with respect to the considered control structure are formulated. Simulation results are presented in Section 3 in order to illustrate the performance of the controller. In Section 4 extensive experimental results are discussed. Section 5 concludes the paper.

2. Controller and observer design

2.1. Dynamics of a perturbed cascaded system

Consider a second order fully actuated control system defined as follows

$$\begin{cases} \dot{x}_1 = x_2, \\ \dot{x}_2 = Bu + h(x_1, x_2) + q(x_1, x_2, u, t), \end{cases} \quad (1)$$

where $x_1, x_2 \in \mathbb{R}^n$ are state variables, $B \in \mathbb{R}^{n \times n}$ is a non-singular input matrix while $u \in \mathbb{R}^n$ stands for an input. Functions $h : \mathbb{R}^{2n} \rightarrow \mathbb{R}^n$ and $q : \mathbb{R}^{3n} \times \mathbb{R}_{\geq 0} \rightarrow \mathbb{R}^n$ denote known and unknown components of the dynamics, respectively. Next, it is assumed that input u in (1) is not directly accessible for a control purpose, however, it is governed by the following first order dynamics

$$\dot{u} = T^{-1}(-u + v), \quad (2)$$

where $v \in \mathbb{R}^n$ is regarded as a real input and $T \in \mathbb{R}^{n \times n}$ is a diagonal matrix of positive time constants. In fact, both dynamics constitute a cascaded third

order plant, for which the underlying component is represented by (1), while (2) corresponds to stable input dynamics.

2.2. Control system design

The control task investigated in this paper deals with tracking of a reference trajectory specified for an output of system (1), (2) which is determined by $y := x_1$. Simultaneously, it is assumed that variables x_2 and u are unavailable for measurement and the only information is provided by the output.

To be more precise, we define at least C^3 continuous reference trajectory $x_d(t) : \mathbb{R}^n \rightarrow \mathbb{R}^n$ and consider output tracking error $\tilde{y} := x_d - x_1$. Additionally, to quantify a difference between u and v , we introduce error $\tilde{u} := v - u$. Since v is viewed as an alternative input of (1), one can rewrite (1) as

$$\begin{cases} \dot{x}_1 = x_2, \\ \dot{x}_2 = Bv - B\tilde{u} + h + q. \end{cases} \quad (3)$$

For control design purposes, the tracking error will be considered with respect to the state of system (3). Consequently, one defines

$$e = \begin{bmatrix} e_1 \\ e_2 \end{bmatrix} := \begin{bmatrix} \tilde{y} \\ \dot{\tilde{y}} \end{bmatrix} = \begin{bmatrix} x_d - x_1 \\ \dot{x}_d - x_2 \end{bmatrix} \in \mathbb{R}^{2n}. \quad (4)$$

Accordingly, taking time derivative of e , one can obtain the following open-loop error dynamics

$$\begin{cases} \dot{e}_1 = e_2, \\ \dot{e}_2 = \ddot{x}_d - Bv + B\tilde{u} - h - q. \end{cases} \quad (5)$$

In order to stabilise system (5) in a vicinity of zero, the following preliminary control law is proposed

$$v := B^{-1} \left(K_p (x_d - \hat{x}_1) + K_d (\dot{x}_d - \hat{x}_2) - h_u + \ddot{x}_d - w_c \right), \quad (6)$$

where $K_p, K_d \in \mathbb{R}^{n \times n}$ are diagonal matrices of constant positive gains, $\hat{x}_1 \in \mathbb{R}^n$, $\hat{x}_2 \in \mathbb{R}^n$ and $w_c \in \mathbb{R}^n$ denote estimates of states and a disturbance, respectively. These estimates are computed by an observer that is not yet defined. Term $h_u : \mathbb{R}^{4n} \rightarrow \mathbb{R}^n$ is a compensation function, designed in attempt to attenuate influence of h on the closed system dynamics, and is defined using available signals as follows

$$h_u := h_1(\hat{x}_1, \hat{x}_2) + h_2(x_d, \dot{x}_d), \quad (7)$$

while h_1 and h_2 satisfy

$$h_1(x_1, x_2) + h_2(x_1, x_2) = h. \quad (8)$$

Next, in order to simplify design of an observer we rewrite dynamics (1). Firstly, we consider a new form which does not introduce any change to the system dynamics and is as follows

$$\begin{cases} \dot{x}_1 = x_2 \\ \dot{x}_2 = Bu + h_u + h - h_u + q. \end{cases} \quad (9)$$

Secondly, according to the active disturbance rejection methodology, it is assumed that

$$z_3 := q + h - h_u \quad (10)$$

describes an augmented state which can be regarded as a total disturbance. Correspondingly, one can introduce extended state $z = [z_1^T \ z_2^T \ z_3^T]^T \in \mathbb{R}^{3n}$, where $z_1 := x_1$ and $z_2 := x_2$. As a result, the following extended form of dynamics (9) can be established

$$\begin{cases} \dot{z}_1 = z_2, \\ \dot{z}_2 = Bu + h_u + z_3, \\ \dot{z}_3 = \dot{q} + \dot{h} - \dot{h}_u. \end{cases} \quad (11)$$

Now, in order to estimate state z we define the following Luenberger-like observer

$$\begin{cases} \dot{\hat{z}}_1 = K_1 (z_1 - \hat{z}_1) + \hat{z}_2, \\ \dot{\hat{z}}_2 = K_2 (z_1 - \hat{z}_1) + \hat{z}_3 + h_u + Bv, \\ \dot{\hat{z}}_3 = K_3 (z_1 - \hat{z}_1), \end{cases} \quad (12)$$

where $\hat{z} = [\hat{z}_1^T \ \hat{z}_2^T \ \hat{z}_3^T]^T \in \mathbb{R}^{3n}$ denotes estimate of z and $K_1, K_2, K_3 \in \mathbb{R}^{n \times n}$ are diagonal matrices of positive gains of the observer which are chosen based on linear stability criteria. Since estimates \hat{z} are expected to converge to real values of z , let observation errors be expressed as $\tilde{z} := z - \hat{z}$. Taking time derivative of \tilde{z} , using (12), (11) and recalling (3) one obtains the following dynamics

$$\dot{\tilde{z}} = H_o \tilde{z} + C_0 B \tilde{u} + C_1 \dot{z}_3 \quad (13)$$

where

$$H_o = \begin{bmatrix} -K_1 & I & 0 \\ -K_2 & 0 & I \\ -K_3 & 0 & 0 \end{bmatrix} \in \mathbb{R}^{3n \times 3n}, \quad (14)$$

$$C_0 = [0 \ -I \ 0]^T, \quad C_1 = [0 \ 0 \ I]^T \in \mathbb{R}^{3n},$$

while I stands for the identity matrix of size $n \times n$. Here, it is required that H_o is Hurwitz, what can be guaranteed by a proper choice of observer gains. Next, we

recall tracking dynamics (5) and feedback (6). It is proposed that compensating term in (6), which partially rejects unknown disturbances, is defined by an estimate provided by observer (12), namely $w_c := \hat{z}_3$. Consequently, by substituting (6) into (5) the following is obtained

$$\dot{e} = H_c e + W_1 \tilde{z} + C_2 B \tilde{u}, \quad (15)$$

where

$$H_c = \begin{bmatrix} 0 & I \\ -K_p & -K_d \end{bmatrix}, \quad W_1 = \begin{bmatrix} 0 & 0 & 0 \\ -K_p & -K_d & -I \end{bmatrix}, \quad C_2 = \begin{bmatrix} 0 \\ I \end{bmatrix} \in \mathbb{R}^{2n \times n} \quad (16)$$

and H_c is Hurwitz for $K_p > 0$ and $K_d > 0$.

Further, in order to facilitate the design and analysis of the closed-loop system, we take advantage of a scaling operator defined by

$$\Delta_m(\alpha) := \text{diag} \{ \alpha^{m-1} I, \alpha^{m-2} I, \dots, I \} \in \mathbb{R}^{mn \times mn}, \quad (17)$$

where $\alpha > 0$ is a positive scalar. Then we define the following scaled tracking and observation errors

$$\bar{e} := (\kappa\omega)^{-1} \Delta_2(\kappa\omega) e, \quad (18)$$

$$\bar{z} := \omega^{-2} \Delta_3(\omega) \tilde{z}, \quad (19)$$

where $\omega \in \mathbb{R}_+$ is a scaling parameter which modifies the bandwidth of the the observer, while $\kappa \in \mathbb{R}_+$ denotes a relative bandwidth of the feedback determined with respect to ω . Embracing this notation one can introduce the following scaled gains

$$\bar{K}_c := (\kappa\omega)^{-1} K_c \Delta_2^{-1}(\kappa\omega), \quad \bar{K}_o := \omega^{-3} \Delta_3(\omega) \begin{bmatrix} K_1^T & K_2^T & K_3^T \end{bmatrix}^T, \quad (20)$$

where $K_c := \begin{bmatrix} K_p & K_d \end{bmatrix} \in \mathbb{R}^{n \times 2n}$. Additionally, exploring relationships (48) outlined in the Appendix, one can rewrite dynamics (15) and (13) as follows

$$\dot{\bar{e}} = \kappa\omega \bar{H}_c \bar{e} + \kappa^{-1} \omega \bar{W}_1 \Delta_3(\kappa) \bar{z} + (\kappa\omega)^{-1} C_2 B \tilde{u}, \quad (21)$$

$$\dot{\bar{z}} = \omega \bar{H}_o \bar{z} + \omega^{-1} C_0 B \tilde{u} + \omega^{-2} C_1 \dot{z}_3, \quad (22)$$

with \bar{H}_c and \bar{H}_o being Hurwitz matrices of forms (16) and (14) defined in terms of scaled gains \bar{K}_c and \bar{K}_o , respectively. Similarly, \bar{W}_1 corresponds to W_1 parameterised by new gains. Since \bar{H}_c and \bar{H}_o are Hurwitz, one can state that the following Lyapunov equations are satisfied

$$\bar{P}_c \bar{H}_c^T + \bar{H}_c \bar{P}_c = -\bar{Q}_c \quad \bar{P}_o \bar{H}_o^T + \bar{H}_o \bar{P}_o = -\bar{Q}_o \quad (23)$$

for some symmetric, positive defined matrices $\bar{Q}_c, \bar{P}_c \in \mathbb{R}^{2n \times 2n}$ and $\bar{Q}_o, \bar{P}_o \in \mathbb{R}^{3n \times 3n}$.

2.3. Stability analysis of the closed-loop cascaded control system

Lyapunov stability of the closed-loop is to be considered now. For this purpose, a state which consists of tracking, observation and input errors is defined as

$$\bar{\zeta} = \begin{bmatrix} \bar{e}^T & \bar{z}^T & \bar{u}^T \end{bmatrix}^T \in \mathbb{R}^{6n}. \quad (24)$$

A positive definite function is proposed as follows

$$V(\bar{\zeta}) = \frac{1}{2} \bar{e}^T \bar{P}_c \bar{e} + \frac{1}{2} \bar{z}^T \bar{P}_o \bar{z} + \frac{1}{2} \bar{u}^T \bar{u}. \quad (25)$$

Its derivative takes form of

$$\begin{aligned} \dot{V}(\bar{\zeta}) = & -\frac{1}{2} \kappa \omega \bar{e}^T \bar{Q}_c \bar{e} - \frac{1}{2} \omega \bar{z}^T \bar{Q}_o \bar{z} + \kappa^{-1} \omega \bar{e}^T \bar{P}_c \bar{W}_1 \Delta_3(\kappa) \bar{z} \\ & + (\kappa \omega)^{-1} \bar{e}^T \bar{P}_c C_2 B \bar{u} + \omega^{-1} \bar{z}^T \bar{P}_o C_o B \bar{u} \\ & + \omega^{-2} \bar{z}^T \bar{P}_o C_1 \dot{z}_3 - \bar{u}^T T^{-1} \bar{u} + \bar{u}^T \dot{v}. \end{aligned} \quad (26)$$

Derivative of control law v defined by (6) can be expressed in terms of $\bar{\zeta}$ as (the details are outlined in the Appendix)

$$\dot{v} = B^{-1} \left(\omega^3 \left(\kappa^3 \bar{K}_c \bar{H}_c \bar{e} + \left(\kappa \bar{K}_c \bar{W}_1 \Delta_3(\kappa) + \bar{W}_2 \Delta_3(\kappa) \bar{H}_o \right) \bar{z} \right) - \dot{h}_u + \ddot{x}_d \right), \quad (27)$$

where $\bar{K}_c := \begin{bmatrix} \bar{K}_p & \bar{K}_d \end{bmatrix} \in \mathbb{R}^{n \times 2n}$ and $\bar{W}_2 := \begin{bmatrix} \bar{K}_c & I \end{bmatrix} \in \mathbb{R}^{n \times 3n}$. Substituting (27) and \dot{z}_3 into (26) leads to

$$\begin{aligned} \dot{V}(\bar{\zeta}) = & -\frac{1}{2} \kappa \omega \bar{e}^T \bar{Q}_c \bar{e} - \frac{1}{2} \omega \bar{z}^T \bar{Q}_o \bar{z} + \kappa^{-1} \omega \bar{e}^T \bar{P}_c \bar{W}_1 \Delta_3(\kappa) \bar{z} \\ & + (\kappa \omega)^{-1} \bar{e}^T \bar{P}_c C_2 B \bar{u} + \omega^{-1} \bar{z}^T \bar{P}_o C_o B \bar{u} + (\kappa \omega)^3 \bar{u}^T B^{-1} \bar{K}_c \bar{H}_c \bar{e} \\ & + \omega^3 \bar{u}^T B^{-1} \left(\kappa \bar{K}_c \bar{W}_1 \Delta_3(\kappa) + \bar{W}_2 \Delta_3(\kappa) \bar{H}_o \right) \bar{z} \\ & - \bar{u}^T T^{-1} \bar{u} + \bar{u}^T B^{-1} \ddot{x}_d + \bar{u}^T B^{-1} \dot{h}_u + \omega^{-2} \bar{z}^T \bar{P}_o C_1 \left(\dot{h} - \dot{h}_u \right) \\ & + \omega^{-2} \bar{z}^T \bar{P}_o C_1 \dot{q}(z_1, z_2, u, t). \end{aligned} \quad (28)$$

In order to simplify the stability analysis, derivative \dot{V} will be decomposed into four terms defined as follows

$$\begin{aligned} Y_1 := & -\frac{1}{2} \kappa \omega \bar{e}^T \bar{Q}_c \bar{e} - \frac{1}{2} \omega \bar{z}^T \bar{Q}_o \bar{z} + \kappa^{-1} \omega \bar{e}^T \bar{P}_c \bar{W}_1 \Delta_3(\kappa) \bar{z} \\ & + (\kappa \omega)^{-1} \bar{e}^T \bar{P}_c C_2 B \bar{u} + \omega^{-1} \bar{z}^T \bar{P}_o C_o B \bar{u} + (\kappa \omega)^3 \bar{u}^T B^{-1} \bar{K}_c \bar{H}_c \bar{e} \\ & + \omega^3 \bar{u}^T B^{-1} \left(\kappa \bar{K}_c \bar{W}_1 \Delta_3(\kappa) + \bar{W}_2 \Delta_3(\kappa) \bar{H}_o \right) \bar{z} - \bar{u}^T T^{-1} \bar{u}, \\ Y_2 := & \bar{u}^T B^{-1} \ddot{x}_d, \quad Y_3 := \bar{u}^T B^{-1} \dot{h}_u + \omega^{-2} \bar{z}^T \bar{P}_o C_1 \left(\dot{h} - \dot{h}_u \right), \\ Y_4 := & \omega^{-2} \bar{z}^T \bar{P}_o C_1 \dot{q}(z_1, z_2, u, t). \end{aligned} \quad (29)$$

Each term of \dot{V} will be now considered separately. Firstly, Y_1 which represents mainly the influence of input dynamics on the nominal system will be looked upon. Negative definiteness of this term will be a starting point for further analysis of the closed-loop stability. Let it be rewritten using the matrix notation as

$$Y_1 = -\frac{1}{2}\omega\bar{\zeta}^T Q_{Y1}\bar{\zeta}, \quad (30)$$

where

$$Q_{Y1} = \begin{bmatrix} \kappa\bar{Q}_c & -\kappa^{-1}\bar{P}_c\bar{W}_1\Delta_3(\kappa) & Q_{Y113} \\ -\kappa^{-1}(\bar{P}_c\bar{W}_1\Delta_3(\kappa))^T & \bar{Q}_o & Q_{Y123} \\ Q_{Y113}^T & Q_{Y123}^T & 2\omega^{-1}T^{-1} \end{bmatrix} \in \mathbb{R}^{6n \times 6n}$$

while

$$\begin{aligned} Q_{Y113} &= -\kappa^{-1}\omega^{-2}\bar{P}_cC_2B - \kappa^3\omega^2(B^{-1}\bar{K}_c\bar{H}_c)^T, \\ Q_{Y123} &= -\omega^{-2}\bar{P}_oC_oB - \omega^2(B^{-1}(\kappa\bar{K}_c\bar{W}_1\Delta_3(\kappa) + \bar{W}_2\Delta_3(\kappa)\bar{H}_o))^T. \end{aligned} \quad (31)$$

It can be showed, that there may exist sets $\Omega_v, K_v \subset \mathbb{R}_+$, such, that for every $\omega \in \Omega_v$ and $\kappa \in K_v$ matrix Q_{Y1} remains positive definite. Domains of both Ω_v and K_v strongly depend on inertia matrix T and input matrix B of nominal system. In the absence of other disturbances the closed-loop system would remain asymptotically stable for such a choice of both ω and κ parameters. Influence of other elements of $\dot{V}(\bar{\zeta})$ will be considered in terms of upper bounds which can be imposed on them.

Assumption 1 Let desired trajectory x_d be chosen such, that norms of $x_d, \dot{x}_d, \ddot{x}_d, \ddot{\ddot{x}}_d$ are bounded by, respectively, constant positive scalar values $x_{b0}, x_{b1}, x_{b2}, x_{b3} \in \mathbb{R}_+$.

Establishing upper bound for norm of Y_2 is straightforward by using Cauchy-Schwartz inequality.

$$\begin{aligned} Y_2 &= -\tilde{u}^T B^{-1} \ddot{\ddot{x}}_d, \\ \|Y_2\| &\leq \|\tilde{u}\| \cdot \|B^{-1} \ddot{\ddot{x}}_d\| \\ &\leq \|\bar{\zeta}\| \|B^{-1}\| x_{b3}. \end{aligned} \quad (32)$$

Now, Y_3 is to be considered. This term comes from imperfect compensation of known dynamics in the nominal (unperturbed) system and it can be further split into the following

$$Y_{31} := \omega^{-2}\bar{z}^T P_oC_1(\dot{h} - \dot{h}_u), \quad Y_{32} := \tilde{u}^T B^{-1}\dot{h}_u. \quad (33)$$

Assumption 2 Let functions $h_1(a, b)$ and $h_2(a, b)$ be defined such, that norms of partial derivatives $\frac{\partial}{\partial a} h_1(a, b)$, $\frac{\partial}{\partial b} h_1(a, b)$, $\frac{\partial}{\partial a} h_2(a, b)$, $\frac{\partial}{\partial b} h_2(a, b)$ are bounded for every $a, b \in \mathbb{R}^n$ by $h_{1a}, h_{1b}, h_{2a}, h_{2b} \in \mathbb{R}_+$ respectively.

By applying chain rule to calculate derivatives of each function and substituting errors \bar{e} , \bar{z} and the desired trajectory for state variables, term Y_{31} can be expressed as

$$\begin{aligned}
 Y_{31} = & \omega^{-2} \bar{z}^T P_o C_1 \left(W_{h1} \begin{bmatrix} \dot{x}_d \\ \ddot{x}_d \end{bmatrix} - W_{h2} \left(\kappa \omega \bar{H}_c \bar{e} + \kappa^{-1} \omega \bar{W}_1 \Delta_3(\kappa) \bar{z} \right. \right. \\
 & \left. \left. + (\kappa \omega)^{-1} C_2 B \bar{u} \right) + W_{h3} \left(\omega \bar{H}_o \bar{z} + \omega^{-1} C_0 B \bar{u} \right) \right), \quad (34)
 \end{aligned}$$

where

$$\begin{aligned}
 W_{h1} &= \left[\left(\frac{\partial h_1}{\partial z_1} + \frac{\partial h_2}{\partial z_1} - \frac{\partial h_2}{\partial x_d} - \frac{\partial h_1}{\partial \hat{z}_1} \right) \left(\frac{\partial h_1}{\partial z_2} + \frac{\partial h_2}{\partial z_2} - \frac{\partial h_2}{\partial \dot{x}_d} - \frac{\partial h_1}{\partial \hat{z}_2} \right) \right], \\
 W_{h2} &= \left[\left(\frac{\partial h_1}{\partial z_1} + \frac{\partial h_2}{\partial z_1} - \frac{\partial h_1}{\partial \hat{z}_1} \right) \kappa \omega \left(\frac{\partial h_1}{\partial z_2} + \frac{\partial h_2}{\partial z_2} - \frac{\partial h_1}{\partial \hat{z}_2} \right) \right], \\
 W_{h3} &= \begin{bmatrix} \frac{\partial h_1}{\partial \hat{z}_1} & \omega \frac{\partial h_1}{\partial \hat{z}_2} & 0 \end{bmatrix}.
 \end{aligned}$$

This term can be said to be bounded by

$$\begin{aligned}
 \|Y_{31}\| \leq & \omega^{-2} \|\bar{\zeta}\| \|P_o C_1\| \left((2h_{1a} + 2h_{2a}) x_{b1} + (2h_{1b} + 2h_{2b}) x_{b2} \right) \\
 & + \|\bar{\zeta}\|^2 \|P_o C_1\| \left(\omega^{-1} \kappa \|W_{h2b}\| \left(\|\bar{H}_c\| + \|\bar{W}_1\| \right) + \omega^{-3} \kappa^{-1} \|W_{h2b}\| \|C_2 B\| \right) \\
 & + \|\bar{\zeta}\|^2 \|P_o C_1\| \left(\omega^{-1} \|W_{h3b}\| \|\bar{H}_o\| + \omega^{-2} \|B\| h_{1b} \right). \quad (35)
 \end{aligned}$$

where $W_{h2b} = [2h_{1a} + h_{2a} \kappa \omega (2h_{1b} + h_{2b})]$ and $W_{h3b} = [h_{1a} \omega h_{1b} \ 0]$. Having established upper bound of Y_{31} , we can perform similar analysis with respect to Y_{32} . Let Y_{32} be rewritten as

$$\begin{aligned}
 Y_{32} = & \bar{u}^T B^{-1} \left(W_{h4} \begin{bmatrix} \dot{x}_d \\ \ddot{x}_d \end{bmatrix} - W_{h5} \left(\kappa \omega \bar{H}_c \bar{e} + \kappa^{-1} \omega \bar{W}_1 \Delta_3(\kappa) \bar{z} + (\kappa \omega)^{-1} C_2 B \bar{u} \right) \right. \\
 & \left. - W_{h6} \left(\omega \bar{H}_o \bar{z} + \omega^{-1} C_0 B \bar{u} \right) \right), \quad (36)
 \end{aligned}$$

where

$$W_{h4} = \left[\left(\frac{\partial h_2}{\partial x_d} + \frac{\partial h_1}{\partial \hat{z}_1} \right) \left(\frac{\partial h_2}{\partial \dot{x}_d} + \frac{\partial h_1}{\partial \hat{z}_2} \right) \right],$$

$$W_{h5} = \begin{bmatrix} \frac{\partial h_1}{\partial \hat{z}_1} & \kappa\omega \frac{\partial h_1}{\partial \hat{z}_2} \end{bmatrix},$$

$$W_{h6} = W_{h3}.$$

An upper bound of norm of Y_{32} can be expressed by the following inequality

$$\begin{aligned} \|Y_{32}\| \leq & \omega^{-2} \|\bar{\zeta}\| \|\bar{P}_o C_1\| (q_{z1} x_{b1} + q_{z2} x_{b2} + \|B\| q_{z2} + \|T^{-1}\| q_u + \|\bar{P}_o C_1\| q_t) \\ & + \kappa\omega^{-1} \|\bar{\zeta}\|^2 \|\bar{P}_o C_1\| \|W_{q2}\| (\|\bar{H}_c\| + \|\bar{W}_1\|) \end{aligned} \quad (37)$$

where $W_{h5b} = [h_{1a} \quad \kappa\omega h_{1b}]$ and naturally $W_{h6b} = W_{h3b}$. A remark can be made now about the structure of W_{h2} , W_{h3} , W_{h4} and W_{h5} . It may be recognized, that elements of these matrices can be divided into groups of derivatives calculated with respect to the first and the second argument. Former of these are not scaled by either observer or regulator bandwidth, while the latter is scaled by either $\kappa\omega$ or ω factor. As will be shown later in the analysis, this difference has a significant influence on the system stability and affects the ability of the controller to reduce tracking errors.

Lastly, some upper bound need to be defined for Y_4 to complete the stability analysis. This final term comes from nominal disturbance $q(z_1, z_2, u, y)$ alone. By the chain rule it can be shown that

$$\begin{aligned} Y_4 = & \omega^{-2} \bar{z}^T \bar{P}_o C_1 \left(W_{q1} \begin{bmatrix} \dot{x}_d \\ \ddot{x}_d \end{bmatrix} + \kappa\omega W_{q2} \bar{H}_c \bar{e} + \kappa^{-1} \omega W_{q2} \bar{W}_1 \Delta_3(\kappa) \bar{z} \right. \\ & \left. + (\kappa\omega)^{-1} W_{q2} C_2 B \bar{u} - \frac{\partial q}{\partial u} T^{-1} \bar{u} + \frac{\partial q}{\partial t} \right), \end{aligned} \quad (38)$$

where $W_{q1} = \begin{bmatrix} \frac{\partial q}{\partial z_1} & \frac{\partial q}{\partial z_2} \end{bmatrix}$ and $W_{q2} = \begin{bmatrix} \frac{\partial q}{\partial z_1} & \kappa\omega \frac{\partial q}{\partial z_2} \end{bmatrix}$.

Assumption 3 Let partial derivatives $\frac{\partial}{\partial z_1} q(z_1, z_2, u, t)$, $\frac{\partial}{\partial z_2} q(z_1, z_2, u, t)$,

$\frac{\partial}{\partial u} q(z_1, z_2, u, t)$, $\frac{\partial}{\partial t} q(z_1, z_2, u, t)$ be defined in the whole domain and let their norms be bounded by constants q_{z1} , q_{z2} , q_u and $q_t \in \mathbb{R}_+$, respectively.

Under Assumption 3 the norm of Y_4 is bounded by

$$\begin{aligned} \|Y_4\| \leq & \omega^{-2} \|\bar{\zeta}\| \|\bar{P}C\| (q_{z1} x_{b1} + q_{z2} x_{b2}) \\ & + \omega^{-1} \|\bar{\zeta}\|^2 \|\bar{P}C W_{5b}\| (\|\bar{H}\| + \omega^{-2} \|\bar{C}B\|) \\ & + \omega^{-2} \|\bar{\zeta}\|^2 \|\bar{P}C\| (\|T^{-1}\| q_u + q_t). \end{aligned} \quad (39)$$

With some general bounds for each of $\dot{V}(\bar{\zeta})$ terms established, conclusions concerning system stability can be finally drawn. For the sake of convenience, let some auxiliary measure of Lyapunov function derivative negative definiteness Λ_V and Lyapunov function derivative perturbation Γ_V be defined as

$$\begin{aligned} \Lambda_V := & \frac{1}{2} \omega \lambda_{\min}(Q_{Y1}) - \kappa \omega \|B^{-1}\| \|W_{h5b}\| (\|\bar{H}_c\| + \|\bar{W}_1\|) \\ & - \omega \|B^{-1}\| \|W_{h6b}\| \|\bar{H}_o\| - 2h_{1b} - \omega^{-1} \|W_{h3b}\| \|\bar{H}_o\| \\ & - \kappa \omega^{-1} \|P_o C_1\| (\|W_{h2b}\| + \|W_{q2}\|) (\|\bar{H}_c\| + \|\bar{W}_1\|) \\ & - \omega^{-2} \|B\| h_{1b} - \omega^{-3} \kappa^{-1} \|W_{h2b}\| \|C_2 B\|, \end{aligned} \quad (40)$$

$$\begin{aligned} \Gamma_V := & \|B^{-1}\| \|(h_{2a} + h_{1a}) x_{b1} + (h_{2b} + h_{1b}) x_{b2}\| \\ & \omega^{-2} \|\bar{P}_o C_1\| (q_{z1} x_{b1} + q_{z2} x_{b2} + \|B\| q_{z2} + \|T^{-1}\| q_u + \|\bar{P}_o C_1\| q_t), \end{aligned} \quad (41)$$

where $\lambda_{\min}(Q)$ stands for the smallest eigenvalue of matrix Q , then upper bound of $\dot{V}(\bar{\zeta})$ can be expressed as

$$\dot{V}_{\bar{\zeta}} \leq -\Lambda_V \|\bar{\zeta}\|^2 + \Gamma_V \|\bar{\zeta}\|. \quad (42)$$

Now, following conditions can be declared

C1 $\omega \in \Omega_v, \kappa \in K_v,$

C2 $\Gamma_V \geq 0,$

and succeeding theorem concludes presented analysis.

Proposition 1 *Perturbed cascade system (1), (2) satisfying Assumptions 1–3, controlled by feedback (6) which is supported by extended state observer (12), remains practically stable if there exist symmetric, positive defined matrices Q_o and Q_c such, that conditions 2.3 and 2.3 can be simultaneously satisfied. Scaled tracking errors $\bar{\zeta}$ are then bounded as follows*

$$\lim_{t \rightarrow \infty} \|\bar{\zeta}(t)\| \leq \frac{\Gamma_V}{\Lambda_V}. \quad (43)$$

Remark 1 *Foregoing proposition remains valid only if Assumptions 1-3 are satisfied. While Assumption 1 considers the desired trajectory only and can be easily fulfilled for any system with state x_1 defined on \mathbb{R}^n , a closer look at the remaining assumptions ought to be taken now. Similar in their nature, both concern imperfectly known parts of the system dynamics, with the difference being whether an attempt to implicitly compensate these dynamics is taken or not. As a known*

dynamic term satisfying Assumption 2 can also be treated as an unknown disturbance, without a loss of generality, only Assumption 3 has to be commented here. It can be noted, that for many commonly considered systems this assumption cannot be satisfied. A mechanical system equipped with revolute kinematic pairs can be an example of such system, which dynamics, due to Coriolis and centrifugal forces, have neither bounded time derivative nor bounded partial derivative calculated with respect to the second state variable. Engineering practice shows nonetheless that for systems, in which cross-coupling is insignificant enough due to a proper mass distribution, this assumption can be approximately satisfied, at least in a bounded set of the state-space, and the stability analysis holds. The requirement that partial derivatives of any disturbance in the system should be bounded is restrictive one, yet less conservative than commonly used in the ADRC analysis expectation of time derivative boundedness. In this sense, the presented analysis is more liberal than ones considered in the literature and it can be expected that enforced assumptions can be better justified.

3. Numerical simulations

In attempt to further research behaviour of the system in the presence of unmodelled dynamics governing the input signal numerical simulations have been conducted. Model of the system has been implemented in Matlab-Simulink environment. The second order, single degree of freedom system and the first order dynamics of the input have been modelled according to the following equations

$$\begin{cases} \dot{x}_1 = x_2, \\ \dot{x}_2 = u, \end{cases} \quad (44)$$

where

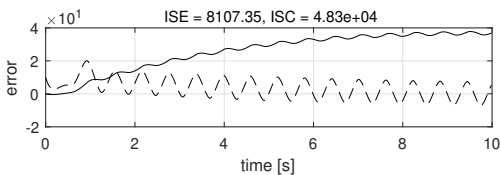
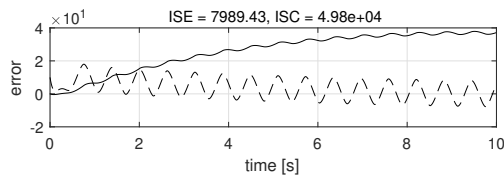
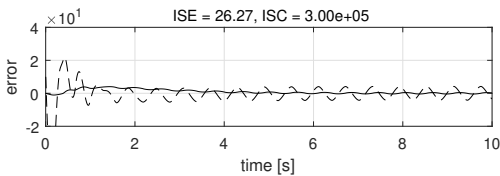
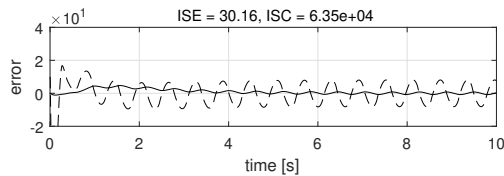
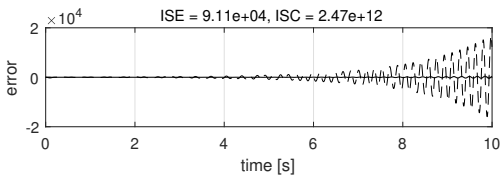
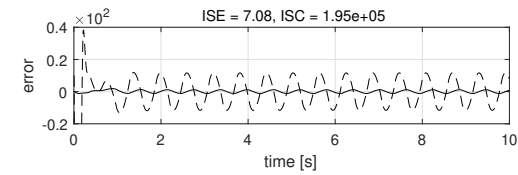
$$\dot{u} = \frac{1}{T} (-u + v) \quad (45)$$

and v is a controllable input of the system. Parameters T and ω of the controller were modified in simulations to investigate how they affect the closed-loop system stability and the tracking accuracy. Chosen parameters of the system are presented in the table 1. Desired trajectory x_d was selected as a sine wave with unitary amplitude and frequency of $\frac{10}{2\pi}$ Hz.

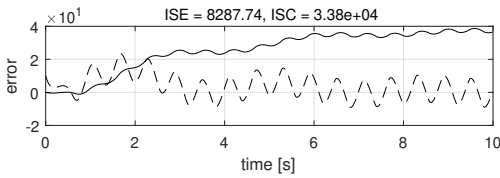
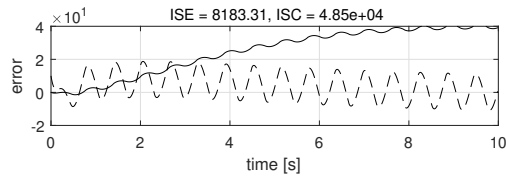
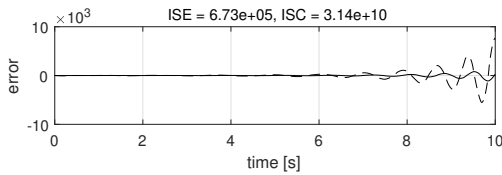
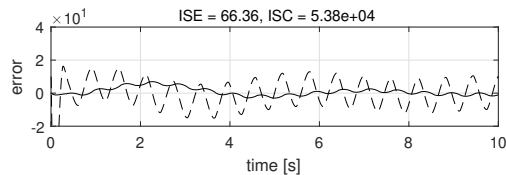
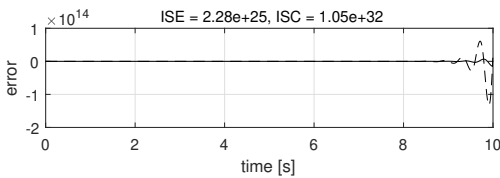
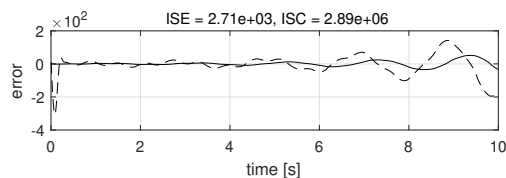
Table 1: Auxiliary gains of the observer and controller

\bar{K}_1	\bar{K}_2	\bar{K}_3	\bar{K}_p	\bar{K}_d	κ
3	3	1	1	2	0.01

Selected results of simulations are presented in Figs. 1–4. Tracking errors of the state variables are presented on the plots. Error of x_1 is presented with solid line, while e_2 has been plotted with dashed lines on each figure. Integrals of squared errors e_1 (ISE criterion) and integral of squared control signals v (ISC criterion) have been calculated for each simulation and are presented above the plots to quantify obtained tracking results. Tests were performed for different values of T and ω , as well as for compensation term $w_c = \hat{z}_3$ enabled or disabled, cf. (6). It can be clearly seen that the existence of some upper bound of Ω is confirmed by simulation results as proposed by Eq. (30). As expected, value of this bound decreases with an increase of time constant T . In the conducted simulations it was not possible to observe and confirm an existence of any lower bound imposed on Ω and for an arbitrarily small ω the stability of the closed-loop system was being maintained. Secondly, an influence of disturbance rejection term \hat{z}_3 is clearly visible and is twofold. For ω chosen to satisfy stability condition 2.3, it can be observed, that the presence of the disturbance estimate allows significant decreasing of tracking errors e_2 caused by the input dynamics which were not modelled during the controller synthesis. Basically, a residual value of error e_2 becomes smaller for a higher value of bandwidth ω . Output error e_1 is also slightly modified, however, this effect is irrelevant according to ISE criterion.

(a) $\omega = 0.1$ (a) $\omega = 0.1$ (b) $\omega = 1$ (b) $\omega = 1$ (c) $\omega = 4$ (c) $\omega = 4$ Figure 1: $T = 0.1$ s, \hat{z}_3 enabledFigure 2: $T = 0.1$ s, \hat{z}_3 disabled

Nonetheless, usage of the disturbance estimate leads to a significant shrink of Ω subset. It is plainly visible, that removal of \hat{z}_3 estimate may lead to recovering of the system stability, cf. Fig. 3 b and Fig. 4 b.

(a) $\omega = 0.1$ (a) $\omega = 0.1$ (b) $\omega = 1$ (b) $\omega = 1$ (c) $\omega = 4$ (c) $\omega = 4$ Figure 3: $T = 1$ s, \hat{z}_3 enabledFigure 4: $T = 1$ s, \hat{z}_3 disabled

4. Experimental results

Practical experiments have been undertaken in order to further investigate the considered control problem. All experiments have been carried out using robotic telescope mount developed at Institute of Automatic Control and Robotics of Poznan University of Technology, [16]. The plant consists of a robotic mount and an astronomic telescope with a mirror of diameter 0.5 m. The robotic mount alone includes two axes driven independently by 24 V permanent magnet synchronous motors (PMSM) with high-precision ring encoders producing absolute position measurement with 32-bit resolution. Control algorithms have been implemented in C++ using Texas Instruments AM4379 Sitara processor with ARM Cortex-A9 core clocked at 600 MHz. Controller itself is implemented in a cascade form which consists of independent current and position loops. Both loops work simultaneously with frequency of 10 kHz. The current loop employs Park-Clark

transformation to express motor dynamics in q - d coordinates. Both q and d auxiliary currents are controlled by independent PI regulators with a static feedforward term and anti-windup correction which are defined as follows

$$\begin{aligned} \dot{v} &= k_i \left(\tilde{i} - k_s \left(k_p \tilde{i} + v + u_r - \text{sat} \left(k_p \tilde{i} + v + u_r \right) \right) \right), \\ u &= \text{sat} \left(k_p \tilde{i} + v + u_r, U_m \right), \end{aligned} \quad (46)$$

where \tilde{i} stands for the current tracking error, v denotes integrator input, u is regulator input, u_r expresses feedforward term, k_p , k_i and k_s are positive gains, and finally $\text{sat}(u^*, U_m)$ the saturation function of signal u^* up to a value of U_m . Output voltage u is generated using PWM technique. Current in d axis is stabilised at zero, while current of q axis tracks the desired current of the axis. For simplicity, a linear relationship between the desired torque and the desired current in q axis is assumed. The corresponding motor constant has been identified experimentally and equals $2.45 \frac{\text{Nm}}{\text{A}}$. The desired torque is computed in the position loop by the active disturbance rejection based controller designed for the second order mechanical system modelled as follows

$$\begin{cases} \dot{x}_1 = x_2 \\ \dot{x}_2 = B\tau + \underbrace{f_c \cdot \tanh(f_t \cdot x_2)}_{h(x_2)}, \end{cases} \quad (47)$$

where $x_1 \in \mathbb{R}^2$ and $x_2 \in \mathbb{R}^2$ are position and velocities of axes, B is input matrix with diagonal coefficients equal $B_{1,1} = \frac{1}{5}$, $B_{2,2} = \frac{1}{30}$, f_c is the constant positive Coulomb friction coefficient while $f_t = 10^3$ expresses scaling term which defines steepness of friction model. Velocity of the axis is approximated in the experiments using either observer estimate \hat{z}_2 or desired trajectory derivative \dot{x}_d . The assumed model of the friction force is strongly local, in the sense that different values of f_c are required for different accelerations in a time instant when the sign of velocity changes. This locality was overcome during the experiments by manual changes of f_c coefficient. While torque generated by the motor is treated as an input signal of the mechanical system, there exist residual dynamics represented by the current loop which is not modelled in the position loop. Here, we assume that these dynamics can be approximated by (2) and thus we can infer about the stability according to mathematical analysis considered in Section 2. Other disturbances come chiefly from flexibility of the mount, ignored cross-coupling reactions between joints and torque ripples generated by synchronous motors. Though some of these disturbances globally do not satisfy assumptions accepted for theoretical analysis of the system stability, in the considered scenario an influence of these dynamics is insignificant. Due to small desired velocities

chosen in the experiment, these assumptions can be approximately satisfied here. All gains of the controllers chosen for experiments are collected in Table 2.

Table 2: Gains of the controllers and observers

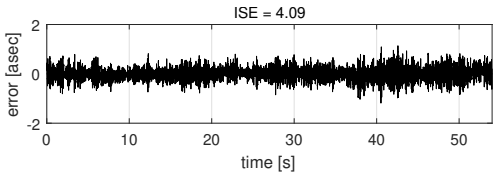
	Horizontal axis	Vertical axis
K_1	$1.2 \cdot 10^3$	$2.4 \cdot 10^2$
K_2	$5.7 \cdot 10^5$	$2.28 \cdot 10^4$
K_3	10^8	$0.8 \cdot 10^6$
K_p	225	225
K_d	24	24

Here we present selected results of the experiments. In the investigated experimental scenarios both axes were at move simultaneously and the desired trajectory was designed as a sine wave with period of 30 s and maximum velocity of $50v_s$, in the first experiment, and $500v_s$, in the second, where $v_s = 7.268 \cdot 10^{-5} \frac{\text{rad}}{\text{s}}$ stands for the nominal velocity of stars on the night sky.

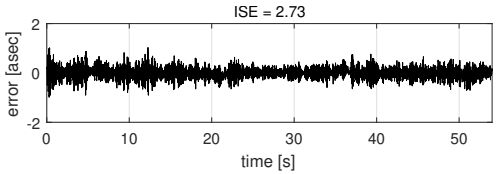
During the system operation significant changes of friction forces are clearly visible and the influence of compensation term can be easily noticed. Since friction terms vary significantly around zero velocity the tracking accuracy is decreased. In such a case the process of the disturbance estimation is not performed fast enough. Furthermore, in the considered application one cannot select larger gains of the observer due to additional dynamics imposed by an actuator and delays in the control loop. Here, one can recall relationship (43) which clearly states that the tracking precision is dependent on the bound of Γ_V , cf. (41). Thus, one can expect that the tracking accuracy increases in operating conditions when disturbances become slow-time varying. Such a property is observed in experiments where friction terms change in a wide range.

Each experiment presents results obtained with different approaches to h_u term design. Once again integral squared error was calculated for each of the presented plots to ease evaluation of the obtained results.

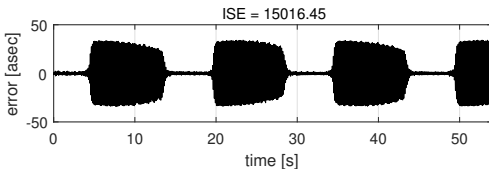
Series of conclusions can be drawn from the presented results. Due to inherently more disturbed dynamics of horizontal axis, any improvement using friction compensation for slow trajectories is hardly achieved. Meanwhile, the compensation term based on the desired trajectory, effectively decreases tracking error bound for all other experiments. As may be expected, compensation function based on estimates of state variables is unable to provide any acceptable tracking quality due to inherent noise in the signal and the existence of input dynamics. It can be noted, that in the first experiment the friction compensation term allows one to decrease the bound of tracking error while overall quality expressed by



(a) $h_u = 0$ (no compensation)

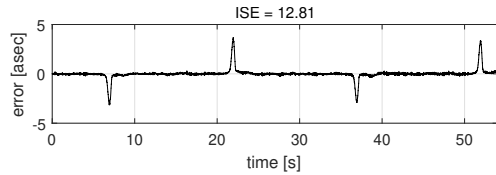


(b) $h_u = 0.5 \cdot \tanh(\dot{x}_d \cdot 10^3)$

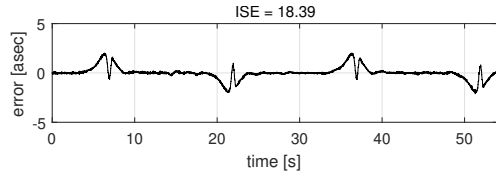


(c) $h_u = 0.5 \cdot \tanh(\hat{z}_2 \cdot 10^3)$

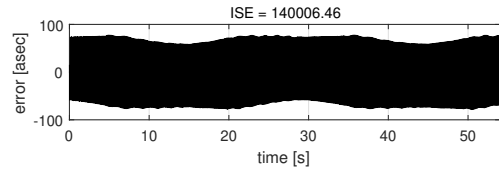
Figure 5: Horizontal axis, first experiment



(a) $h_u = 0$ (no compensation)

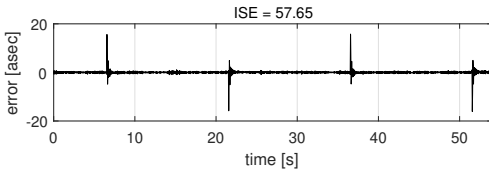


(b) $h_u = 0.5 \cdot \tanh(\dot{x}_d \cdot 10^3)$

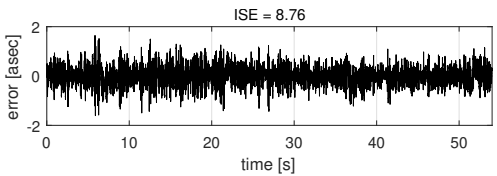


(c) $h_u = 0.5 \cdot \tanh(\hat{z}_2 \cdot 10^3)$

Figure 6: Vertical axis, first experiment

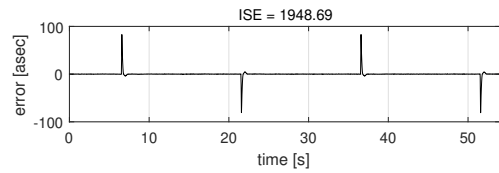


(a) $h_u = 0$ (no compensation)

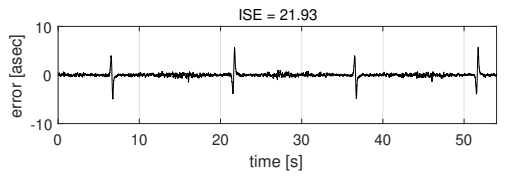


(b) $h_u = 0.15 \cdot \tanh(\dot{x}_d \cdot 10^3)$

Figure 7: Horizontal axis, second experiment



(a) $h_u = 0$ (no compensation)



(b) $h_u = 0.15 \cdot \tanh(\dot{x}_d \cdot 10^3)$

Figure 8: Vertical axis, second experiment

ISE criterion is worse in comparison to this obtained in the experiment without the corresponding term in the feedback. This behaviour is not seen in the second experiment, in which significant improvement was obtained for both axes in terms of error boundary as well as ISE criterion.

5. Conclusions

This paper is focused on the application of ADRC controller to a class of second order systems subject to differentiable disturbances. In particular, the system is analysed taking into account the presence of the first order input dynamics and unmodelled terms which may include cross-coupling effects between the state variables. By the means of Lyapunov analysis, general conditions of practical stability are discussed. It is proved that, even in the presence of additional input dynamics, boundedness of partial derivatives of total disturbance can be a sufficient requirement to guarantee stability of the closed-loop system.

Using numerical simulations the considered controller is compared against a simple PD-based regulator. The obtained results confirm that in the case of input dynamics, the bandwidth of an extended observer is limited which restricts the effectiveness of the ADRC approach. Lastly, practical results of employing ADRC regulator in the task of trajectory tracking for a robotised astronomical telescope mount are presented. In this application, it is assumed that friction effects are modelled inaccurately and a local drive control-loop is treated as unknown input dynamics. The obtained results illustrate that the considered control algorithm can provide a high tracking accuracy.

Further research in this topic may include attempts to explore in more details conditions for the feasible selection of the observer parameters in order to guarantee the stability of the closed-loop system. Other forms of input dynamics and observer models can also be considered in the future works.

A. Appendix

A.1. Selected properties of scaled dynamics

Assuming that errors and gains are scaled according to (18), (19) and (20) the following relationships are satisfied:

$$\begin{aligned} \Delta_2(\kappa\omega)H_c\Delta_2^{-1}(\kappa\omega) &= \kappa\omega\overline{H}_c, & \Delta_3(\omega)H_o\Delta_3^{-1}(\omega) &= \omega\overline{H}_o, \\ \Delta_2(\kappa\omega)W_1 &= W_1, & W_1\Delta_3^{-1}(\omega) &= \overline{W}_1\Delta_3(\kappa), & W_2 &= \Delta_3(\kappa\omega)\overline{W}_2. \end{aligned} \quad (48)$$

A.2. Computation of \dot{v}

Taking advantage of estimate \bar{z} and assuming that $w_c := \hat{z}_3$ one can rewrite (6) as follows

$$v = B^{-1} \left(K_c e + K_c \begin{bmatrix} \tilde{z}_1^T \\ \tilde{z}_2^T \end{bmatrix}^T - h_u + \ddot{x}_d - \hat{z}_3 \right), \quad (49)$$

where $K_c := [K_p \ K_d]$. Equivalently, one has

$$v = B^{-1} (K_c e - W_2 \tilde{z} - h_u + \ddot{x}_d - \dot{z}_3). \quad (50)$$

Consequently, time derivative of v satisfies

$$\begin{aligned} \dot{v} &= B^{-1} (K_c \dot{e} + W_2 \dot{\tilde{z}} - \dot{h}_u + \ddot{x}_d - \dot{z}_3) \\ &\stackrel{(15),(13)}{=} B^{-1} (K_c H_c e + K_c W_1 \tilde{z} + K_c C_2 B \tilde{u} + W_2 H_o \tilde{z} \\ &\quad + W_2 C_o B \tilde{u} + W_2 C_1 \dot{z}_3 - \dot{z}_3 - \dot{h}_u + \ddot{x}_d) \\ &= B^{-1} (K_c H_c e + K_c W_1 \tilde{z} + W_2 H_o \tilde{z} - \dot{h}_u + \ddot{x}_d). \end{aligned} \quad (51)$$

A.3. Computations of Y_3 and Y_4

By chain rule it can be shown that

$$\begin{aligned} \dot{h}_1(z_1, z_2) &= \begin{bmatrix} \frac{\partial h_1}{\partial z_1} & \frac{\partial h_1}{\partial z_2} \end{bmatrix} \begin{bmatrix} \dot{x}_d \\ \dot{x}_d \end{bmatrix} - \begin{bmatrix} \frac{\partial h_1}{\partial z_1} & \kappa \omega \frac{\partial h_1}{\partial z_2} \end{bmatrix} \dot{\tilde{e}}, \\ \dot{h}_2(z_1, z_2) &= \begin{bmatrix} \frac{\partial h_2}{\partial z_1} & \frac{\partial h_2}{\partial z_2} \end{bmatrix} \begin{bmatrix} \dot{x}_d \\ \dot{x}_d \end{bmatrix} - \begin{bmatrix} \frac{\partial h_2}{\partial z_1} & \kappa \omega \frac{\partial h_2}{\partial z_2} \end{bmatrix} \dot{\tilde{e}}, \end{aligned} \quad (52)$$

$$\dot{h}_1(\hat{z}_1, \hat{z}_2) = \begin{bmatrix} \frac{\partial h_1}{\partial \hat{z}_1} & \frac{\partial h_1}{\partial \hat{z}_2} \end{bmatrix} \begin{bmatrix} \dot{x}_d \\ \dot{x}_d \end{bmatrix} - \begin{bmatrix} \frac{\partial h_1}{\partial \hat{z}_1} & \kappa \omega \frac{\partial h_1}{\partial \hat{z}_2} \end{bmatrix} \dot{\tilde{e}} - \begin{bmatrix} \frac{\partial h_1}{\partial \hat{z}_1} & \omega \frac{\partial h_1}{\partial \hat{z}_2} & 0 \end{bmatrix} \dot{\tilde{z}}, \quad (53)$$

$$\dot{h}_2(x_d, \dot{x}_d) = \begin{bmatrix} \frac{\partial h_2}{\partial x_d} & \frac{\partial h_2}{\partial \dot{x}_d} \end{bmatrix} \begin{bmatrix} \dot{x}_d \\ \dot{x}_d \end{bmatrix}.$$

From here, following are true

$$\dot{h} - \dot{h}_u = W_{h1} \begin{bmatrix} \dot{x}_d \\ \dot{x}_d \end{bmatrix} - W_{h2} \dot{\tilde{e}} + W_{h3} \dot{\tilde{z}}, \quad \dot{h}_u = W_{h4} \begin{bmatrix} \dot{x}_d \\ \dot{x}_d \end{bmatrix} - W_{h5} \dot{\tilde{e}} - W_{h6} \dot{\tilde{z}}, \quad (54)$$

what leads to solution of Y_3 by means of basic substitution.

Now, the computation of term Y_4 will be taken into account. Disturbance term $q(z_1, z_2, u, t)$ can be expressed in form of

$$\begin{aligned} \dot{q}(z_1, z_2, u, t) &= \frac{\partial q}{\partial z_1} (\dot{x}_d - \dot{e}_1) + \frac{\partial q}{\partial z_2} (\dot{x}_d - \dot{e}_2) + \frac{\partial q}{\partial u} T^{-1} (-u + v) + \frac{\partial q}{\partial t} \\ &= W_{q1} \begin{bmatrix} \dot{x}_d \\ \dot{x}_d \end{bmatrix} + W_{q2} \dot{\tilde{e}} - \frac{\partial q}{\partial u} T^{-1} \tilde{u} + \frac{\partial q}{\partial t} \\ &= W_{q1} \begin{bmatrix} \dot{x}_d \\ \dot{x}_d \end{bmatrix} + W_{q2} (\kappa \omega \overline{H}_c \tilde{e} + \kappa^{-1} \omega \overline{W}_1 D(\kappa) \tilde{z} + (\kappa \omega)^{-1} C_2 B \tilde{u}) \\ &\quad - \frac{\partial q}{\partial u} T^{-1} \tilde{u} + \frac{\partial q}{\partial t}. \end{aligned} \quad (55)$$

References

- [1] C. AGUILAR-IBANEZ, H. SIRA-RAMIREZ, and J.A. ACOSTA: Stability of active disturbance rejection control for uncertain systems: A Lyapunov perspective. *International Journal of Robust and Nonlinear Control*, **27**(18), (2017), 4541–4553.
- [2] G. BARTOLINI, A. FERRARA, and E. USAI: Chattering avoidance by second-order sliding mode control. *IEEE Transactions on Automatic Control*, **43**(2), (1998), 241–246.
- [3] G. BARTOLINI, L. FRIDMAN, A. PISANO, and E. USAI, editors: *Modern sliding mode control theory. New perspectives and applications*, volume 37 of *LNCIS*. Springer-Verlag, 2008.
- [4] A. BARTOSZEWICZ: Time-varying sliding modes for second-order systems. *IEE Proc. on Control Theory and Applications*, **143** (1996), 455–462.
- [5] I. CASTILLO, L. FRIDMAN, and J.A. MORENO: Super-twisting algorithm in presence of time and state dependent perturbations. *International Journal of Control*, **91**(11), (2018), 2535–2548.
- [6] Z. CHEN, Q. ZHENG, and Z. GAO: Active disturbance rejection control of chemical processes. In *2007 IEEE International Conference on Control Applications*, pages 855–861, Oct 2007.
- [7] M. FLIESS and C. JOIN: Model-free control and intelligent PID controllers: Towards a possible trivialization of nonlinear control? 15th IFAC Symposium on System Identification, *IFAC Proceedings Volumes*, **42**(10), (2009), 1531–1550.
- [8] M. FLIESS and C. JOIN: Model-free control. *International Journal of Control*, **86**(12), (2013), 2228–2252.
- [9] M. GALICKI: Finite-time control of robotic manipulators. *Automatica*, **51** (2015), 49–54.
- [10] M. GALICKI: Finite-time trajectory tracking control in a task space of robotic manipulators. *Automatica*, **67** (2016), 165–170.
- [11] Z. GAO: From linear to nonlinear control means: A practical progression. *ISA Transactions*, **41**(2), (2002), 177–189.
- [12] Z. GAO: Active disturbance rejection control: a paradigm shift in feedback control system design. In *2006 American Control Conference*, pages 2399–2405, June 2006.

- [13] J. HAN: Auto-disturbance rejection control and its applications. *Control and Decision*, **13**(1), (1998) (in Chinese).
- [14] J. HAN: From PID to Active Disturbance Rejection Control. *IEEE Transactions on Industrial Electronics*, **56**(3), (2009), 900–906.
- [15] H.K. KHALIL and L. PRALY: High-gain observers in nonlinear feedback control. *International Journal of Robust and Nonlinear Control*, **24**(6), (2014), 993–1015.
- [16] K. KOZŁOWSKI, D. PAZDERSKI, B. KRYSIAK, T. JEDWABNY, J. PIASEK, S. KOZŁOWSKI, S. BROCK, D. JANISZEWSKI, and K. NOWOPOLSKI: High precision automated astronomical mount. In R. Szweczyk, C. Zieliński, and M. Kaliczyńska, editors, *Automation 2019. Advances in Intelligent Systems and Computing*, volume 920. Springer, 2020.
- [17] A. LEVANT: Sliding order and sliding accuracy in sliding mode control. *International Journal of Control*, **58**(6), (1993), 1247–1263.
- [18] A. LEVANT: Robust exact differentiation via sliding mode technique. *Automatica*, **34**(3), (1998), 379–384.
- [19] R. MADOŃSKI and P. HERMAN: Survey on methods of increasing the efficiency of extended state disturbance observers. *ISA Transactions*, **56** (2015), 18–27.
- [20] R. MIKLOSOVIC and Z. GAO: A dynamic decoupling method for controlling high performance turbofan engines. 16th IFAC World Congress, *IFAC Proceedings Volumes*, **38**(1), (2005), 532–537.
- [21] A. NOWACKA-LEVERTON, M. MICHAŁEK, D. PAZDERSKI, and A. BARTOSZEWICZ: Experimental verification of smc with moving switching lines applied to hoisting crane vertical motion control. *ISA transactions*, **51** (2012), 682–693.
- [22] P. NOWAK, K. STEBEL, T. KŁOPOT, J. CZECZOT, M. FRĄTCZAK, and P. ŁASZCZYK: Flexible function block for industrial applications of active disturbance rejection controller. *Archives of Control Sciences*, **28**(3), (2018), 379–400.
- [23] S. SHAO and Z. GAO: On the conditions of exponential stability in active disturbance rejection control based on singular perturbation analysis. *International Journal of Control*, **90**(10), (2017), 2085–2097.

- [24] B. SUN and Z. GAO: A dsp-based active disturbance rejection control design for a 1-kw h-bridge dc-dc power converter. *IEEE Transactions on Industrial Electronics*, **52**(5), (2005), 1271–1277.
- [25] V. UTKIN: Variable structure systems with sliding modes. *IEEE Trans. on Automatic Control*, **22** (1977), 212–222.
- [26] D. WU, K. CHEN, and X. WANG: Tracking control and active disturbance rejection with application to noncircular machining. *International Journal of Machine Tools and Manufacture*, **47**(15), (2007), 2207–2217.